Fermi surface and electronic density of states of molybdenum*

D. D. Koelling, F. M. Mueller, and A. J. Arko
Argonne National Laboratory, Argonne, Illinois 60439

J. B. Ketterson
Argonne National Laboratory, Argonne, Illinois 60439
and Department of Physics, Northwestern University, Evanston, Illinois 60201

(Received 1 April 1974)

The electronic energy-band structure of molybdenum has been calculated by means of the relativistic augmented-plane-wave method applied to the overlapping charge-density model. Full Slater exchange was employed. Calculations of extremal calipers, extremal cross-sectional areas, and cyclotron effective masses for the magnetic field along symmetry directions are reported and compared with experimental data where available. Comparison of the theoretical and experimental cyclotron-mass data indicate an anisotropic electron-phonon mass enhancement of approximately 0.33, which is smaller than the McMillan value of 0.41.

I. INTRODUCTION

The electronic structure of the chromium-group metals (Cr, Mo, W) has continued to be of interest to research workers. Several years ago Lomer[1] introduced a model for the Fermi surface of these elements based on the augmented-plane-wave (APW) band-structure calculations on iron performed by Wood.[2] This surface consists of four sheets: (i) The largest surface, which arises from the fourth band, is the electron jack centered at the point Γ of the Brillouin zone (BZ); (ii) the next largest surface is the third-band hole octahedron at H; (iii) the six nearly ellipsoidal third-band hole surfaces at the N points; (iv) the smallest surfaces which are the six electron fifth-band lenses located on the Δ line. The Fermi surface of molybdenum has been studied experimentally by the de Haas–van Alphen (dHvA) effect,[3–7] radio-frequency size effect (RFSE),[8,9] magnetoacoustic geometric resonance (FR),[10,11] and cyclotron resonance (CR).[12] The results of these investigations are in qualitative agreement with the Lomer model. First-principles APW band-structure calculations for molybdenum were performed by Loucks[13] and Mattheiss.[14] More recently, Kim and Buyers[15] and separately Iverson and Hodges[16] performed calculations using interpolating schemes; Petroff and Viswanathan[17] carried out APW calculations and Christensen did a relativistic APW (RAPW) calculation.[18] The Fermi surface of Mo was recently parameterized[19] by fitting the dHvA data of Hoekstra and Stanford[6] to a nonspherical muffin-tin model for the potential using a relativistic generalization of the Green's-function formalism of John, Lehmann, and Ziesche.[20]

What remains to be understood in the electronic structure of molybdenum (and many other transition metals) are those properties in which the wave functions play a significant role. Except for calculations of the photoemission spectrum by Petroff and Viswanathan[17] and the Compton profiles by Kim and Buyers[15] little has yet been attempted in this direction for transition metals, primarily due to computational costs. Two areas which we feel deserve special attention are the well-known phonon-anomalies of the Mo-Nb system[21] together with the related superconducting transition temperature T_c,[22] and the use of molybdenum as a host to study impurity and defect structures (the latter will be the subject of a future publication[23]). The multiplicity of Fermi-surface sheets, the high-percentage d-like character, and low density of states at the Fermi energy makes such studies in molybdenum especially attractive; molybdenum is one of the few transition metals with an electronic-specific-heat coefficient comparable to noble or simple metals.

In this paper we consider the electronic band structure of molybdenum by means of RAPW calculations. Before embarking on elaborate calculations of these properties requiring wave functions, it was felt that a detailed comparison of the band-structure results with the empirical Fermi-surface data was essential. Moreover, recent RFSE caliper data of Boiko *et al.*[8] and Cleveland and Stanford[9] and the dHvA data of Hoekstra and Stanford[6] were substantially more complete than previous work. In addition, the approximately 5% differences (far greater than the combined experimental errors reported) between the two sets of caliper measurements required theoretical examination; especially important was the larger gap reported[9] between the jack and octahedron, since this implied a spin-orbit splitting some three times larger than the $4d$ atomic value for molybdenum. Other workers[24] had found that such spin-orbit splittings, at least in the calculations, rather closely follow the atomic values.

The plan of this paper is as follows: Sec. II

briefly reviews the RAPW method; Sec. III presents and discusses our results; and Sec. IV draws our conclusions.

II. RELATIVISTIC-AUGMENTED-PLANE-WAVE METHOD

The APW method, as conceived by Slater[25] in 1937, has been extended to include relativistic effects by a number of workers.[26] In this form the method has been successfully applied to the electronic structure of noble, transition, and actinide metals and compounds. The periodic potential is factorized within a unit cell into two regions: inside and outside a sphere whose radius was comparable to, but less than, a Wigner-Seitz radius—the so-called "muffin-tin radius." Outside the sphere the potential was averaged and then assumed constant; inside it was assumed to be spherically symmetric. Because of its shape, this approximation has been called the "muffin-tin" (MT) approximation by Ziman, and because of its simplicity and high accuracy, it has been almost universally utilized. One of the advantages of the RAPW method compared with the Korringa-Rohn-Rostoker or Green's-function band-structure technique[27] is the ease with which the corrections to the muffin-tin form may be included in the secular equation—the so-called warped-muffin-tin (WMT) approximation. (It involves exactly the same operations to include the nonspherical potential terms inside the spheres.) Basically the "outside" potential is expanded in a Fourier series

$$V_{\text{out}}(\vec{r}) = \sum_{\vec{K}} V(\vec{K})\, e^{i\vec{K}\cdot\vec{r}} \ , \tag{1}$$

where V_{out} is constructed to be zero inside the muffin-tin spheres. Because the RAPW's *are* simply plane waves in the external or interstitial part of the cell, the matrix elements are readily found[28] to be

$$\langle \vec{k}s \,|\, H^{\text{WMT}} - E \,|\, \vec{k}'s' \rangle = \langle \vec{k}s \,|\, H^{\text{MT}} - E \,|\, \vec{k}'s \rangle + \langle s \,|\, s' \rangle\, V(\vec{k} - \vec{k}') \ . \tag{2}$$

Table I lists the first 10 matrix elements $V(K)$ (ordered by length). Generally the matrix elements of higher $\vec{K}$ are small (of the order of or less than 1 mRy), except for those associated with the "large" [100] direction.

The potential chosen was derived from the usual overlapping charge-density model, and a $4d^5 5s^1$ configuration was assumed. Because of the importance of the spin-orbit effect on the Fermi surface of molybdenum the d portion of the potential was constructed from a mixed-spin orbital: Two states were assumed to be $4d^{3/2}$, three were $4d^{5/2}$, and, finally, one state was $5s^{1/2}$. In this way the small difference between the two spin-orbit-split radial wave functions was made approximately self-consistent. Table I shows that if we represent the splitting at Γ approximately as a tight-binding derived spin-orbit splitting,[29] then the value of ξ is similar to an atomic spin-orbit splitting. As Andersen has discussed,[30] this splitting (viewed this way) is also $\vec{k}$-dependent. At no place in the BZ would the tight-binding spin-orbit approximation be greatly in error.

TABLE I. Parameters for RAPW calculation.

a	5.9468 a.u.	lattice constant
c	$4d^5 5s^1$	assumed atomic configuration
R	2.5551 a.u.	muffin-tin radius
ξ atomic	0.0072 Ry	atomic spin-orbit splitting $(4d) = 2[E(l+\frac{1}{2}) - E(l-\frac{1}{2})]/(2l+1)$
ξ band	0.0073 Ry	band spin orbit $= \frac{2}{5}(\Gamma_{7+} - \Gamma_{8+})$
1	$V[000]$	−1.78 mRy
2	$V[220]$	−1.33 mRy
3	$V[400]$	+7.95 mRy
4	$V[422]$	+0.12 mRy
5	$V[440]$	−1.45 mRy
6	$V[620]$	−3.65 mRy
7	$V[444]$	−1.81 mRy
8	$V[642]$	+1.88 mRy
9	$V[800]$	+4.21 mRy
10	$V[660]$	+0.69 mRy

III. RESULTS AND DISCUSSION

The RAPW method and the potential of the last section were used to find the energy bands along the principal symmetry directions. The results for the lowest six bands are given in Fig. 1 and are qualitatively similar to previously published work with a relatively broad and free electron like s-p band intersecting and hybridizing with a d-band complex. The small shifts due to the MT potential compared with the WMT potential were too small to be seen clearly on this scale and so are not presented. The Fermi energy (discussed below) intersects the band structure several times along the symmetry directions, but, counting from the lowest level Γ_{6+}, does not intersect bands 1 or 2 at all; bands 3–5 comprise the Fermi surface.

In addition to the points along the symmetry directions, the lowest six energy bands were found on a $\pi/4a$ mesh and at an additional set of $\vec{k}$ points at body-centered sites near the Fermi surface, so that a total of 94 independent points in $\frac{1}{48}$ of the BZ were found. These were then fit with a Fourier series of the form

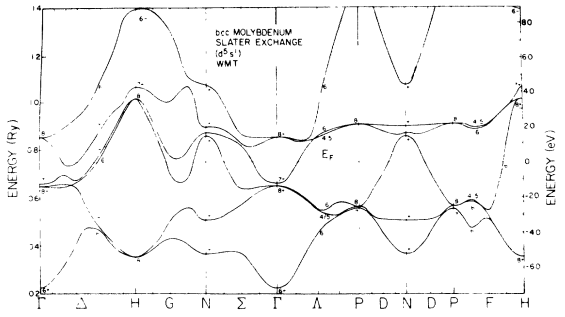

FIG. 1. Relativistic-augmented-plane-wave energy bands of molybdenum along high-symmetry directions calculated for the warped-muffin-tin approximation to the overlapping atomic-charge-density model.

$$E_n(\vec{k}) = \sum_{\vec{R}} C_{\vec{R}}^n e^{i\vec{k}\cdot\vec{R}} \tag{3}$$

using a least-squares matrix-inversion procedure.[31] All the C's of a given star of $\vec{R}$ are equal, and the sets are ordered by the length of $\vec{R}$. The truncation of (3) at 58 stars gave rms errors of 1.8, 2.5, 3.5, 2.9, 3.2, and 9.0 mRy for bands 1–6, respectively. Band 6 has the largest error, primarily because of the slow convergence of the Fourier series in the vicinity of the points H and P. This reflects the rapid variation of the sixth band in these regions and also the fact that the sixth band is much wider than bands 2–5. The quality of the fit of the important bands 3 and 4 in the vicinity of the Fermi energy is gratifying but not too important; the relevant quantity (for Fermi-surface work) is the fractional error $\Delta k/k$, where, if we assume $E \propto k^2$, $\Delta k/k = \frac{1}{2}\Delta E/E$. If E is the bandwidth, about 0.4 Ry, then ΔE should be of order or less than 2–4 mRy, so that $\Delta k/k$ is of order (1–2)%. This is consistent with our truncation of (3). Left out of this analysis is the poorness of the fit near points of discontinuous first derivative, such as crossing points along symmetry lines. We argue that the amount of phase space where such considerations are important is, with 58 stars, rather microscopic (a volume of essentially the inverse of the cube of the shortest "wavelength" employed), and can be neglected in determining the density of states and Fermi energy. Such crossing points could produce systematic errors in determining the Fermi surface, however.

The Fourier series was then used to calculate the density of states by QUAD-LINEAR, a program similar to the one discussed by Cooke and Wood.[32] A quadratic approximation was made to the Fourier representation over a cubic cell of size $(2\pi/a)/(2m+1)$, where m was a parameter. The quadratic fit was then approximated by linear sections (planes) oyer subregions, the size of which was governed by the criterion that either the quadratic error of the linear approximation be less than one third a histogram width or the number of subregions be less than 15^3 in any one (small) cubic cell. In order to establish a convergence criterion two types of critical structures were examined: peaks in the density of states such as those occuring at 0.433 and 0.508 Ry in bands 1 and 2, respectively, and shoulders (places of large first derivative) such as 0.473 and 0.533 Ry. Table II lists these as a function of the quadratic subdivision parameter m. High accuracy requires that this parameter be at least 19 (21 was used in the results below). The time listed is the total CPU (central processing unit) time on the IBM 360/75/195 in the Applied Mathematics Division of Argonne National Laboratory, including compilation and the determination of the Fourier coefficients (both short). The long and constant times for low MESH (at first glance, paradoxical) are caused by the automatic choice of the size of the linearization region, as discussed above. The final choice of $m = 19$ is similar to, but somewhat more stringent than, that discussed by Janak.[33] In any event we regard 400 sec as being acceptably small for a density of states accurate (we estimate) to better than 0.1% near the critical points (worst case) on an energy grid of 2.5-mRy spacing. The $m = 21$ density of states is plotted in Fig. 2 and is similar to those of Mattheiss[14]; Petroff and Viswananthan,[17] and Gupta and Sinha,[34] but with somewhat sharper structure.

The Fermi energy was found from either the criterion that the total number of states should be six electrons per atom or the criterion that the electron and hole volumes should be equal (Mo is a compensated metal). It is important to note, because there seems to be some confusion about the point in the literature, that in the absence of numerical error these criteria are identical. We denote the volume of the occupied part of the nth band by e_n and of the unoccupied part of the band by h_n. For convenience we suppress the energy argument. By including the phase-space density factor these

TABLE II. Convergence of QUAD-LINEAR density of states with MESH parameter for critical structure (worst case) of the two lowest bands. Units of energy are rydbergs and units of density of states are (states)/Ry atom.

	Time	Band 1		Band 2	
m	(sec)	$E_1 = 0.433$	$E_2 = 0.473$	$E_3 = 0.508$	$E_4 = 0.533$
5	353	19.338	20.107	13.813	39.416
7	353	17.550	17.703	12.853	34.776
9	353	19.374	19.508	12.168	32.018
11	353	19.380	18.227	11.390	32.405
13	358	19.379	18.649	11.511	31.336
15	367	19.154	18.606	11.026	31.265
17	369	18.896	18.438	10.908	30.748
19	380	18.776	19.019	11.140	30.730
21	400	18.809	18.347	11.195	30.787

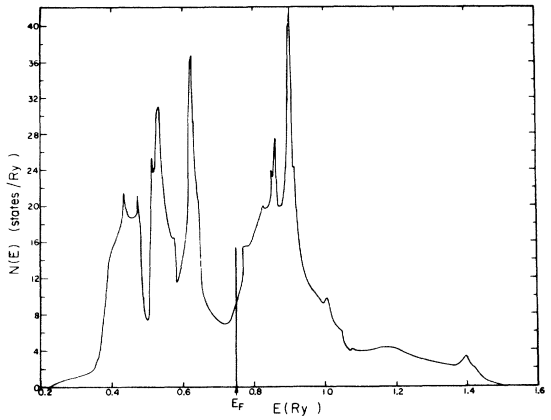

FIG. 2. Density of states of molybdenum for the lowest six bands.

volumes can be put in units of the states per atom enclosed by a surface, so

$$h_n = 2 - e_n \quad . \tag{4}$$

Then the integrated density of states criterion is

$$e_1 + e_2 + e_3 + e_4 + e_5 + e_6 = 6 \quad . \tag{5}$$

But, as bands 1 and 2 are full ($e_1 = e_2 = 2$) and band 6 is empty ($e_6 = 0$), this becomes

$$e_3 + e_4 = 2 - e_5 = h_5 \quad , \tag{6}$$

which is the volume-compensation result. The equivalence of the two techniques is seen when it is observed that the density of states is normally calculated by determining $e_n(E)$ and using the result

$$n_n(E) = \frac{de_n}{dE} \quad . \tag{7}$$

The only place where the precision might be different between the two methods is if one were to perform the derivative in Eq. (7) and then integrate back to the e_n.

Table III lists these volume results. The actual Fermi energy was found by fitting a quadratic form ($V_T = A + BE + CE^2$) to the four points closest to a volume of two electrons per atom and solving $V_T(E) = 6$ for $E = E_F$. Of course, this Fermi energy

TABLE III. Volume and density of states by band at the Fermi energy.

Band	Volume [(states)/(unit) cell]	Density [(states)/Ry atom]
3 (all hole contributions)	−0.2023	2.78
4 (jack)	0.1928	4.99
5 (lenses)	0.0095	0.91
4+5 (electron contribution)	0.2023	4.90
(3+4+5) (total)	0	8.68

0.7465 Ry gave compensation as well. The total density of states and that of each subband was found from $n(E) = (dV/dE)_{E=E_F} = B + 2CE_F$. This procedure, since it averages over several neighboring values, is more accurate than a simple linear interpolation. Surprising is the large density of states [0.91 (states)/(atom) Ry] for the rather small [0.0095 (electron)/(atom)] fifth-band-lens sheet. This merely emphasizes the low overall density of states of sheets 3 and 4 rather than the especially high density of states of sheet 5.

The Fermi surface was found from solutions to $E_n(\vec{k}) = E_F$, where, because of the possibility of systematic crossing errors in the Fourier series discussed above, the RAPW Hamiltonian itself was used to compute the dHvA orbits, using orbit-tracing routines designed to obtain the dHvA areas by Simpson's-rule integration.[35] For the four-ball ($\vec{H} \parallel [100]$) and two-ball ($\vec{H} \parallel [110]$) jack orbits, the Fermi radius vector is multivalued for some directions in the plane of the orbit. In such cases the standard Simpson's-rule integration technique (using the angular increment $d\theta$) is not feasible and one must resort to the slightly less accurate trapezoidal rule with constant arc length. The orbit-tracing routines were extended to handle the multivalued case.[36] To permit the analytical computation of $\vec{\nabla}_{\vec{k}} E$ (necessary for orbit tracing and computing the cyclotron mass using the Hellmann-Feynman technique[37]), the analytical derivatives of the elements of the RAPW secular matrix were calculated. Figure 3 plots our results for the (100) and (110) cross sections of the Fermi surface of Mo. The areas and effective masses for the magnetic field along symmetry directions are listed in Table V. Typically, one orbital area required one to two minutes of CPU time on the Argonne IBM 360/75/195, depending on the grid (usually $\sim 2\frac{1}{2}°$) and the angular range required by symmetry.

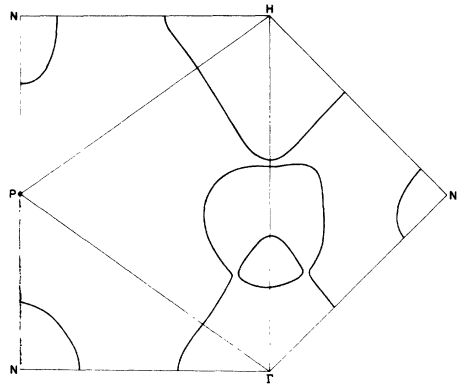

FIG. 3. Cross sections of the Fermi surface of molybdenum in the (1, 0, 0) and (1, 1, 0) planes.

TABLE IV. Fermi-surface caliper dimensions (in $Å^{-1}$). To obtain dimensions in $2\pi/a$ units divide entries in table by 1.9966.

	Direction	This work	Loucks[a]	RFSE[b]	RFSE[c]	dHvA[d]
Band 3						
Octahedron	[100]	0.81	0.84	0.79	0.75	0.81
(hole)	[110]	0.60	0.63	0.60	0.58	0.61
	[111]	0.50	0.53	0.51	0.48	0.49
	[112]	0.54	•••	0.54	0.51	0.52
N-ellipsoid	*NP*	0.40	0.37	0.38	0.35	0.37
(hole)	*NF*	0.36	0.27	0.29	0.32	0.33
	NH	0.22	0.19	0.22	0.20	0.22
Band 4						
Jack (electron)	[100]	1.15	1.15	1.16	1.10	
	[110]	0.52	0.49	0.52	•••	
	[111]	0.46	0.44	0.47	0.44	
	[112]	0.50		0.49		
Band 5						
Δ-lens (electron)	[100]	0.26	•••	0.31	0.24	
(diam)	[110]	0.35	•••	•••	•••	
Jack-octahedron separation						
	[100]	0.04	•••	0.05 ± 0.04	•••	0.050

[a]See Ref. 13.
[b]See Ref. 8.
[c]See Ref. 8.
[d]See Ref. 9.

The Fermi-surface calipers along high-symmetry directions are listed in Table IV and compared with Loucks's calculations (now some 10 years old) and with several sets of experimental data.[8,9] The overall agreement between all sources, considering the diversity of results and techniques represented here, must be considered remarkable. (Although we have not made any use of the technique in this paper, it is clear that the agreement of Table IV provides substantial justification for the use of an *ab initio* technique such as the RAPW method to represent the Fermi surface in terms of a few parameters such as phase shifts.[19]) We have included in Table IV the derived caliper dimensions of Hoekstra and Stanford[6] for the easily inverted centrosymmetric sheets, but not for the more difficult jack. (We prefer to consider the dHvA data by itself below.) Our conclusion regarding the jack-octahedron separation is, nevertheless, the same as Hoekstra and Stanford[6] and, separately, Iverson and Hodges[16] (namely, about 2% of the Γ-*H* distance), in agreement with the conclusion of Boiko *et al.*[8] Thus the RAPW calculations presented here support the idea that this gap is spin-orbit controlled and that this spin-orbit splitting is consistent with the atomic 4*d* spin-orbit splitting of molybdenum (see Table I). Because of the parallelism of the bands observed along the [001] direction, this conclusion is not governed by, for example, the accuracy of the placement of the Fermi level itself.

In Table V we consider the orbital-area data of Hoekstra and Stanford[9] (in atomic units) compared with RAPW calculations. The agreement between the calculated and experimental areas of about 1.2% is gratifying and strongly supports the assumption that one can accurately predict Fermi-surface dimensions using the single-particle approximation. Although we do not present the results here, we have also performed these calculations in the muffin-tin approximation. The resulting areas agreed equally well with the experimental areas. Based on this criterion alone, one would conclude that the two models were indistinguishable. This is not surprising, based on the evidence[38] that it is the nonspherical contributions to the potential inside the spheres which are a major correction to the muffin-tin approximation for the bcc transition metals. The WMT masses, however, are (1–5)% larger for the electron jack, 4% larger for the lenses, 1.5% larger for hole octahedron, and (1–3)% smaller for the hole ellipsoids. Thus the inclusion of the non-muffin-tin terms in the interstitial region has had an effect. The nonspherical terms inside the muffin-tin spheres would have a comparable effect. This ef-

TABLE V. Extremal areas (a.u.), cyclotron effective masses, and enhancement factors.

Orbit	Field direction	Origin	Experimental area	Calculated area ($E_F = 0.7465$ Ry)	Calculated mass	Experimental mass	Enhancement factor λ
Jack	[001]	(0, 0, 0)	0.6174[a]	0.6282	2.781	3.85[d]	0.39
Jack	[111]	(0, 0, 0)	0.2264[a]	0.2254	0.779	0.99[c]	0.26
Jack	[110]	(0, 0, 0)	0.4223[a]	0.4313	1.738	2.55[d]	0.47
Jack neck	[100]		0.0313[a]	0.0370	0.409	0.541[c]	0.33
Ball	[100]		0.0846[a]	0.0914	0.639		
Lens	[110]	(0, 0, 0.3)	0.0137[a]	0.0170	0.253	0.29[b]	0.15
Octahedron	[001]	(0, 0, 1)	0.4023[a]	0.4110	−0.925	1.22[c]	0.32
						1.27[d]	0.37
Octahedron	[110]	(0, 0, 1)	0.3031[a]	0.3085	−0.661	0.88[c]	0.33
						0.90[d]	0.36
Octahedron	[111]	(0, 0, 1)	0.2767[a]	0.2823	−0.555	0.72[c]	0.30
Ellipsoid	[001]	$(\frac{1}{2}, \frac{1}{2}, 0)$	0.0607[a]	0.0685	−0.304	0.396[b]	0.30
						0.37[d]	0.22
Ellipsoid	[110]	$(\frac{1}{2}, \frac{1}{2}, 0)$	0.0703[a]	0.0804	−0.363	0.43[i]	0.18
Ellipsoid	[110]	$(\frac{1}{2}, \frac{1}{2}, 0)$	0.0974[a]	0.1166	−0.432	0.57[c]	0.32
						0.52[i]	0.20
rms error[e]				1.2%			

[a] Hoekstra and Stanford, Ref. 6.
[b] Lever and Myers, Ref. 5.
[c] Arko, Ref. 7.
[d] Herman (Ref. 12) or Herman and Kruger (Ref. 12).
[e] rms error definition employed is $[\sum_i (A_i^{\text{expt}} - A_i^{\text{calc}})^2]^{1/2} / [\sum_i (A_i^{\text{expt}})^2]^{1/2}$. Ball and neck orbits of the jack are not included.

fect, however, is, on the average, too small to seriously affect the derived mass enhancements considered below.

The fact that the over-all error is relatively small in our unadjusted calculation is again a strong support for the validity of the band approach. As Christensen[18] has pointed out, the success may be based on the low density of states of molybdenum near the Fermi level. We could slightly improve the agreement by adjusting the density-of-states derived Fermi level by 1 mRy or so, for example. Because the bands used in the Fourier interpolation scheme had inaccuracies of the order 2–3 mRy, the density-of-states derived Fermi energy could be inaccurate by 1 mRy. We have not done this because the spirit of the present investigation was to test the validity of an unparametrized band model rather than to provide a best fit to the experimental Fermi-surface data. (In addition, it is not clear that the small shifts would be physically significant.)

The calculated cyclotron effective masses are listed in Table V; also included are the experimental masses measured by Leaver and Myers,[5] Arko,[7] and Hermann and Kruger.[12] Because of the variations in the reported experimental masses, it is not possible to make a precise statement concerning the magnitude and anisotropy of the electron-phonon mass enhancement factor λ; the orbital average of this quantity is defined such that $(1 + \lambda_m) m_{\text{BS}} = m^*$. A value of $\lambda_m \cong 0.35$ seems to be indicated for the larger sheets [jack (0.33) and octahedron (0.38)]; smaller values are found for the lens (0.15) and ellipsoid (0.24) sheets. The average value of λ over the entire Fermi surface may be determined from our calculated total density of states $N(E_F) = 8.68$ (states)/(atom) Ry and the measured electronic specific heat.[39,40] Roser, Onn, and Meyer[39] obtain the value 1.83 mJ/mole K^2, which corresponds to an enhanced total density of states $N_\lambda = 10.55$ (states)/(atom) Ry. If we define the Fermi-surface average of λ such that $(1 + \lambda_T) N(E_F) = N_\lambda$ we obtain a value $\lambda_T = 0.22$. This value of λ_T is much smaller than that found from the McMillan theory.[41] According to this theory,

$$\lambda = \frac{1.04 + \mu^* \ln(\Theta/1.45 T_c)}{(1 - 0.62\,\mu^*) \ln(\Theta/1.45 T_c) - 1.04} , \tag{8}$$

where μ^*, the Coulomb pseudopotential parameter, is defined as

$$\mu^* = \frac{(1 - 2\alpha)^{1/2}}{\ln(\Theta/1.45 T_c)} ; \tag{9}$$

for molybdenum, the transition temperature $T_c = 0.92$ K the characteristic phonon frequency $\Theta = 460$ K, and the isotope-shift parameter $\alpha = 0.37 \pm 0.04$ lead to $\mu^* = 0.09$ and $\lambda = 0.41$.

We do not believe that the anisotropy we find between the sheets is a severe criticism of the single-parameter (λ) theory of McMillan. As Allen and Cohen[42] have discussed, it is perfectly feasible

that some regions of phase space will have a larger and some a smaller electron-phonon coupling. The transition temperature, as a bulk thermodynamic quantity, would still depend on an average λ; to the extent that the λ anisotropy is small, this parameter is an electron-phonon coupling; if large it is just another representation of the transition temperature.

More puzzling is the over-all difference of 0.41 compared with 0.22. Because of the logarithmic dependences, the value of λ in the McMillan formula does not depend sensitively on Θ or μ^*. For example $\mu^* = 0.13$ was used in deriving the value of 0.41 (Table III of Ref. 41); replacing this by $\mu^* = 0.09$ (Table II of Ref. 41—the isotope value) reduces the λ to 0.35. The strong-coupling correction $(1+0.62\lambda)/(1+\lambda)$, which is approximately 0.9 for $\lambda \sim 0.3$, was neglected by McMillan in making his estimate of μ^*, but also does not change a μ^* derived self-consistently by much ($\mu_s^* = 0.086$). Thus the difference between the enhancement of the specific heat γ and the orbital masses is larger than our estimate of the intrinsic accuracy of the McMillan λ (about 0.1). The close relation between the bcc electronic structure of niobium (used to derive the McMillan equation) and molybdenum, and the general overall and historical success of the theory make it unlikely that the McMillan λ of 0.41 is very inaccurate.

The electronic density of states and the values quoted in Table III can be imprecise for several reasons: misplacement of the Fermi energy; error in the model potential; error introduced by the muffin-tin or warped muffin tin approximation; error in the shape of the bands in the vicinity of the Fermi energy due to the inadequacy of the Fourier-series representation; and inaccuracy of the QUADLINEAR integration scheme due to the quadratic-linear approximation. This last error we estimate at 0.1% at most. This misplacement error we believe is small both because the minimal shape in the total density of states is rather independent of the number of Fourier terms (a much less accurate density of states based on fewer expansion coefficients gave 8.0 states per Ry and a similar minimal shape) and because of the extrinsic accuracy of the bands as shown by the comparison given in Table IV. In order to reduce the band density of states to a value consistent with $10.5/1.4 = 7.5$ states per Ry, the Fermi energy would need to be lowered by some 25 mRy, destroying the agreement of the bands with the areas in Table IV. The model-potential error should not be large owing to the observed insensitivity at the Fermi energy. And the changes caused by including the WMT approximation indicate that the muffin-tin approximation causes errors too small and of the wrong sign to account for the effect. The error in the model potential we estimate from the change in the bandwidth of niobium[43] between two calculations: full Slater exchange, $\alpha = 1$, non-self-consistent (0.755); Kohn-Sham-Gaspar, $\alpha = \frac{2}{3}$, self-consistent (0.673). This yields a change of about 12%. If we assume that Mo is similar to Nb and that the density of states varies as the inverse bandwidth, then this range of variation is too small to explain the λ discrepancies above. Additional corroborating evidence for the correctness of the bandwidth of present calculations is given in the good agreement with optical properties in Ref. 44.

The other element is the cited[39] γ value of 1.83. An examination of the original paper by Roser *et al.* shows that this value is lower than a cluster of historical values around 2.1 mJ/mole K^2. The value of Roser *et al.* is now accepted because they showed that the γ value is quite sensitive to the purity of the sample; a specimen with a residual resistance ratio (RRR) of >1600 had $\gamma = 1.81$, while a sample whose RRR was 313 had $\gamma = 1.89$. This sensitivity can be understood if the impurity has a virtual state near the Fermi level with a width sufficiently broad to sample the higher density of states on both sides of the narrow minimum seen in the single-particle density of states shown in Fig. 2. Of course the alloy has a higher γ than pure Mo in this model.

The cyclotron effective-mass data definitely favor a λ value greater than 0.22. For the electron jack and hole octahedron the microwave cyclotron resonance measurements of Herrmann and Krueger yield enhancement factors as large as 0.47 and 0.37, respectively. The majority of the density of states is contributed by these two sheets of the surface. A simple weighted average over all sheets yields a cyclotron-mass derived λ of about 0.33.

IV. CONCLUSIONS

The band model has been shown to provide an accurate representation of the Fermi surface of molybdenum. Puzzling is the disagreement found here between the McMillan λ of 0.41, the band and specific-heat derived value of 0.22, and the cyclotron "average" of 0.33. We believe that it is critical to remeasure the electronic specific heat of molybdenum on extremely pure samples whose resistivity ratio is greater than ~5000 (easily available nowadays) and on Mo with controlled amounts of dilute interstitial impurities (O, C, N, and B). The historical γ values of about 2.1 mJ/mole K^2 remove the discrepancy. The previous conclusion[6,16] that the jack-octahedron gap is approximately 2.7% of the Γ-to-H distance and related to an atomic spin-orbit splitting is supported by the band calculations presented here.

ACKNOWLEDGMENTS

We wish to acknowledge Professor S. Doniach, Professor A. J. Freeman, Professor T. Geballe; Dr. F. Fradin, Dr. G. S. Knapp, Dr. H. Myron, Dr. B. W. Veal, and Dr. R. S. Viswanathan for helpful discussions; H. Sowers for assistance on the octahedron mass measurements reported here, S. Katilavas for computational assistance; Tom Kirkman for the use of his reentrant Fermi-surface program; and the Computer Center of the Applied Mathematics Division of Argonne National Laboratory for excellent service.

---

*Work performed under the auspices of the U.S. Atomic Energy Commission.

[1]W. M. Lomer, Proc. Phys. Soc. Lond. 80, 489 (1962).
[2]J. H. Wood, Phys. Rev. 126, 517 (1962).
[3]G. B. Brandt and J. A. Rayne, Phys. Rev. 132, 1945 (1963).
[4]D. M. Sparlin and J. A. Marcus, Phys. Rev. 144, 848 (1966).
[5]G. Leaver and A. Myers, Philos. Mag. 19, 465 (1969).
[6]J. A. Hoekstra and J. L. Stanford, Phys. Rev. B 8, 1416 (1973).
[7]A. J. Arko (unpublished).
[8]V. V. Boiko, V. A. Gasparov, and I. G. Gverdtsiteli, Zh. Eksp. Teor. Fiz. 56, 489 (1969) [Sov. Phys.-JETP 29, 267 (1969)]; V. V. Boiko and V. A. Gasparov, *ibid.* 61, 1976 (1971) [*ibid.* 34, 1054 (1972)].
[9]J. R. Cleveland and J. L. Stanford, Phys. Rev. B 4, 311 (1971).
[10]C. K. Jones and J. A. Rayne, Phys. Lett. 8, 155 (1964); in *Proceedings of the Ninth International Conference on Low Temperature Physics* (Plenum, New York, 1965), p. 790.
[11]P. A. Bezuglyi, S. E. Zhevago, and V. I. Denisenko, Zh. Eksp. Teor. Fiz. 49, 1457(1965) [Sov. Phys.-JETP 22, 1002 (1966)].
[12]R. Herrmann, Phys. Status Solidi 25, 427 (1968); R. Herrmann and H. Krueger, Phys. Status Solidi 41, 99 (1971).
[13]T. L. Loucks, Phys. Rev. 139, A1181 (1965).
[14]L. F. Mattheiss, Phys. Rev. 139, A1893 (1965).
[15]S. M. Kim and W. J. L. Buyers, Can. J. Phys. 50, 1777 (1972).
[16]R. J. Iverson and L. Hodges, Phys. Rev. B 8, 1429 (1973).
[17]I. Petroff and C. R. Viswanathan, Phys. Rev. B 4, 799 (1971).
[18]N. E. Christensen, *Computational Methods in Solid State Physics*, edited by F. Herman, N. N. Dalton, and T. R. Koehler (Plenum, New York, 1972), p. 155.
[19]J. B. Ketterson, D. D. Koelling, J. C. Shaw, and L. R. Windmiller, Phys. Rev. B (to be published).
[20]Yu. M. Demkov and V. S. Rudakov, Zh. Eksp. Teor. Fiz. 59, 2035 (1970); [Sov. Phys.-JETP 32, 1103 (1971)]; W. John, G. Lehmann, and P. Ziesche, Phys. Status Solidi. B 53, 287 (1972).
[21]Y. Nakagawa and A. D. B. Woods, Phys. Rev. Lett. 11, 271 (1968).
[22]J. K. Hulm and R. D. Blaugher, AIP Conf. Proc. 4, 1 (1972), and the references contained therein.
[23]H. W. Myron, F. M. Mueller, and D. D. Koelling (unpublished).
[24]F. M. Mueller, A. J. Freeman, J. O. Dimmock, and A. M. Furdyna, Phys. Rev. B 1, 4617 (1970); L. Hodges, H. Ehrenreich, and N. D. Lang, Phys. Rev. 152, 505 (1966).
[25]J. C. Slater, Phys. Rev. 51, 151 (1937).
[26]For a description of the RAPW method see T. L. Loucks, *The Augmented Plane Wave Method* (Benjamin, New York, 1967) and the references and reprints contained therein.
[27]J. Korringa, Physica (Utr.) 13, 392 (1947); W. Kohn and N. Rostoker, Phys. Rev. 94, 1111 (1954); B. Segall and F. J. Ham, Methods Comput. Phys. 8, 251 (1968).
[28]D. D. Koelling, A. J. Freeman, and F. M. Mueller, Phys. Rev. B 1, 1318 (1970).
[29]J. Friedel, P. Lenglart, and G. Leman, J. Phys. Chem. Solids 25, 781 (1964); L. F. Mattheiss and R. E. Watson, Phys. Rev. Lett. 13, 526 (1964); F. Herman and S. Skillman, *Atomic Structure Calculations* (Prentice-Hall, Englewood Cliffs, N. J., 1963).
[30]O. K. Andersen, Ph.D. thesis (Technical University, Lyndby, Denmark, 1969) (unpublished); Phys. Rev. B 2, 1883 (1970).
[31]R. Maglic and F. M. Mueller, Int. J. Magn. 1, 512 (1971).
[32]J. F. Cooke and R. F. Wood, Phys. Rev. B 5, 1276 (1972); G. Gilat and L. J. Raubenheimer, Phys. Rev. 144, 390 (1966).
[33]J. F. Janak, *Computational Methods in Band Theory*, edited by P. M. Marcus, J. F. Janak, and A. R. Williams (Plenum, New York, 1971), p. 323.
[34]R. P. Gupta and S. Sinha, Phys. Rev. B 3, 2401 (1971).
[35]J. B. Ketterson, F. M. Mueller, and L. R. Windmiller, Phys. Rev. 186, 656 (1969); B. Bosacchi, J. B. Ketterson, and L. R. Windmiller, Phys. Rev. B 4, 1197 (1971).
[36]T. Kirkman (unpublished).
[37]J. C. Shaw, J. B. Ketterson, and L. R. Windmiller, Phys. Rev. B 5, 3894 (1972).
[38]G. S. Painter, J. S. Faulkner, and G. M. Stocks, Phys. Rev. B 9, 2448 (1974).
[39]D. C. Roser, D. G. Onn, and Horst Meyer, Phys. Rev. 138, A1661 (1965).
[40]H. L. Luo, R. S. Viswanathan, and J. Engelhardt, in *Proceedings of the Thirteenth International Conference on Low Temperature Physics, Boulder, Colo.*, 1972, edited by R. H. Kropschat and K. D. Timmerhaus (University of Colorado Press, Boulder, Colo., 1973). These authors find a value $\gamma = 1.75$ mJ/K^2.
[41]W. McMillan, Phys. Rev. 167, 331 (1968); K. H. Bennemann and J. W. Garland, AIP Conf. Proc. 4, 103 (1972).
[42]P. Allen and M. L. Cohen (private communication).
[43]J. R. Anderson, D. A. Papconstantopoulos, J. W. McCaffrey, and J. E. Schirber, Phys. Rev. B 7, 5115 (1973).
[44]D. D. Koelling, F. M. Mueller, and B. W. Veal, Phys. Rev. B (to be published).